CHAPTER

TIGHT GAS SANDSTONE RESERVOIRS, PART 1: OVERVIEW AND LITHOFACIES

14

Y. Zee Ma[1], W.R. Moore[1], E. Gomez[1], W.J. Clark[1], Y. Zhang[2]
Schlumberger, Denver, CO, USA[1]; *University of Wyoming, Laramie, WY, USA*[2]

14.1 INTRODUCTION AND OVERVIEW

Although shale gas plays have been in the spotlight recently, natural gas in tight sandstones is actually also an important hydrocarbon resource. In many cases, tight gas sandstone resources can be developed more easily than shale gas reservoirs as the rocks generally have higher quartz content, and are more brittle and easier to complete for production.

This chapter first gives an overview of evaluating tight gas sandstone reservoirs, including their depositional environments, and other reservoir characteristics. Then, it presents an integrated methodology for lithofacies analysis and modeling. Because identification of lithofacies and rock typing is a key to characterizing these types of reservoirs (Rushing et al., 2008), we discuss lithofacies classification using wireline logs. We present methods on how to populate the lithofacies data from wells to a three-dimensional (3D) model while discussing the advantages and disadvantages of each method for modeling tight gas formations.

The next chapter is the second part of tight gas sandstone reservoirs, in which petrophysical analysis, formation evaluation, and 3D modeling of petrophysical properties are presented.

14.1.1 BACKGROUND

Tight gas sandstone reservoirs are natural extensions of conventional sandstone reservoirs, but with lower permeability and generally lower effective porosity. Hydrocarbons have traditionally been produced from sandstone and carbonate reservoirs with high porosity and permeability. Sandstone reservoirs with permeability lower than 0.1 milliDarcy (mD) were historically not economically producible, but advances in stimulation technology have enabled production from these tight formations. There is some confusion regarding the definition of tight gas sandstone reservoirs; they are sometimes referred to as deep-basin, basin-centered gas accumulation, or pervasive sandstone reservoirs (Meckel and Thomasson, 2008). The United States Gas Policy Act of 1978 classified tight gas formations as those that have in situ permeability less than 0.1 mD (Kazemi, 1982). Thus, sandstone gas reservoir in which the formation has average permeability lower than 0.1 mD is a tight gas play regardless of its depositional environment. These reservoirs can occur in numerous settings, including channelized fluvial systems (e.g., the Greater Green River basin, Law, 2002; Shanley, 2004; Ma et al., 2011), alluvial fans,

Unconventional Oil and Gas Resources Handbook. http://dx.doi.org/10.1016/B978-0-12-802238-2.00014-6
Copyright © 2016 Elsevier Inc. All rights reserved.

delta fan, slope and submarine fan channels deposits (e.g., Granite Wash, Wei and Xu, 2015), or shelf margin (e.g., Bossier sand, Rushing et al., 2008), among others. Some tight gas sandstones contain different depositional facies; the Cotton Valley formation, for example, includes stacked shoreface/barrier bar deposits, tidal channel, tidal delta, inner shelf, and back-barrier deposits. Because of the variety of depositional environments for sandstones and other variations, there is no typical tight gas sandstone reservoir (Holditch, 2006a). While drilling, well design, and completion techniques for producing a tight sandstone reservoir are often similar to producing a shale gas reservoir, exploration and resource evaluation for them generally are quite different (Kennedy et al., 2012).

Tight gas production was first developed in the San Juan Basin of the western United States; large-scale development of tight gas sandstone reservoirs has a longer history than large-scale development of shale gas reservoirs. Approximately 1 trillion cubic feet (Tcf) was produced per year by 1970 in the United States (Naik, 2003). Meckel and Thomasson (2008) distinguished three periods of evolution for the evaluation and production of tight gas sandstone reservoirs: preparadigm period (1920–1978), paradigm period (1979–1987), and mop-up period (1988–present). The paradigm period was marked by Master's article (1979), arguing the extensive existence of hydrocarbon resources in tight formations. Many of the basins that contain gas in tight sandstones in North America have already been in exploration or production phase, playing an important role in the North American energy equation. In fact, as clastic formations are found in many parts of the world, tight gas sands make up an important resource worldwide. Rogner (1997) has estimated the worldwide tight gas resource to be approximately 7500 Tcf, but other estimates carry a much larger number for tight gas plays (Naik, 2003). In comparison, the worldwide shale gas resource has been estimated to be 16,100 Tcf (Rogner, 1997).

14.1.2 BASIN-CENTERED EXTENSIVE DEPOSITS OR CONVENTIONAL TRAPS

Two schools of thought exist regarding the geologic control of tight gas sandstone reservoirs: continuous basin-centered gas accumulations or BCGAs (Law, 2002; Schmoker, 2005), and gas accumulation in low-permeability tight sandstones of a conventional trap (Shanley et al., 2004). The difference between these two theories can have a huge impact on the strategy for gas exploration in tight sandstones and the estimate of worldwide gas resources in these formations (Aguilera and Harding, 2008).

As a matter of fact, conventional traps represent more limited, favorable structural and/or stratigraphic setups that enable natural gas accumulation after its generation and migration. They are thus rather geologically circumstanced. On the other hand, the BCGA theory implies a continuous basin-wide gas accumulation, or at least widely spread within a basin. Law (2002) argued that BCGAs contained extremely large gas resources, and were one of the more economically viable unconventional gas resources, but there was generally a poor understanding of BCGAs despite a significant body of work on defining characteristics of gas-saturated reservoirs. These include studies in the deep basin of Alberta, the San Juan basin of New Mexico and Colorado by Masters (1979), and the Greater Green River basin and Great Divide basin of the western United States (Law and Spencer, 1989; Law, 1984; Spencer, 1989). According to Law (2002), the BCGA must meet the following five criteria (Camp, 2008): (1) large regional extent, measuring tens of miles in diameter; (2) low permeability, less than 0.1 mD; (3) abnormal pressure (either overpressured or underpressured); (4) gas saturated; and (5) absence of downdip water contacts. Figure 14.1 illustrates the

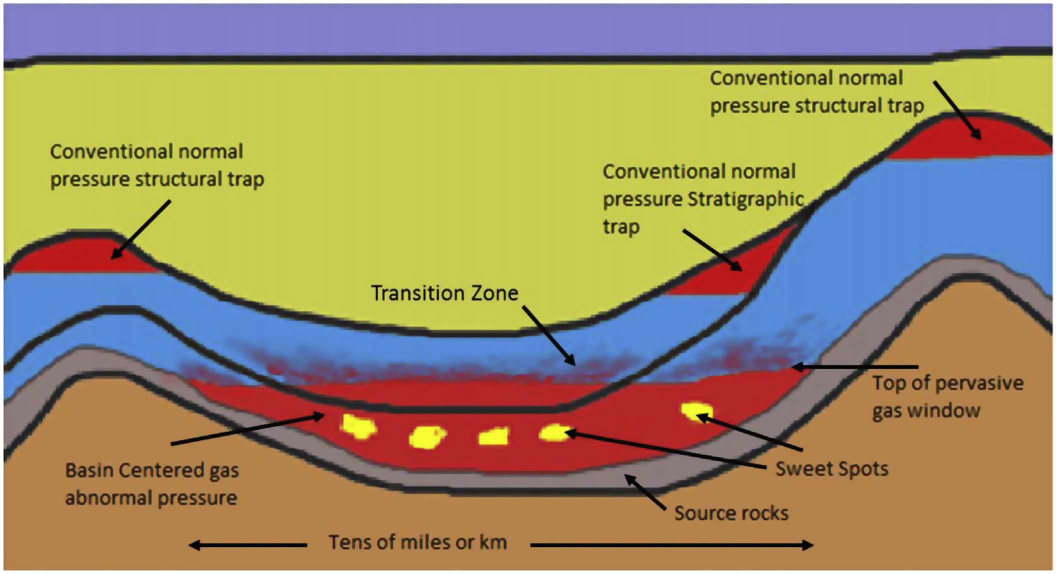

FIGURE 14.1

A schematic cross-section view illustrating BCGA model.

Modified from Schenk and Pollastro (2002).

main characteristics of BCGS theory. One important characteristic in this theory is that the trapping mechanism is a diffused capillary-pressure seal instead of conventional structural or stratigraphic controls.

Shanley et al. (2004) argued that low-permeability reservoir systems such as those found in the Greater Green River basin were not examples of BCGAs, and they suggested that only truly continuous-type gas accumulations were to be found in hydrocarbon systems in which gas entrapment was dominated by adsorption. Studies on several tight gas sandstone reservoirs in the Greater Green River Basin have suggested that subtle structural and stratigraphic traps better explain the primary controls for the hydrocarbon accumulations (Camp, 2008).

14.1.3 GENERAL PROPERTIES OF TIGHT GAS SANDSTONE RESERVOIRS

Although the two theories, the BCGA and conventional trapping mechanism, have significant differences regarding the exploration strategies of tight gas sandstone reservoirs, none of them denies the importance of formation evaluation in any given tight gas play.

14.1.3.1 Source rock

Source rock is important for all hydrocarbon resource accumulations. For tight gas sands, the source rock should be in proximity to the relatively porous deposit so that the expulsion can drive the gas into the porous formation and form the reservoir (Meckel and Thomasson, 2008). The total organic carbon of the source rock should be large enough for generation of a significant amount of hydrocarbon.

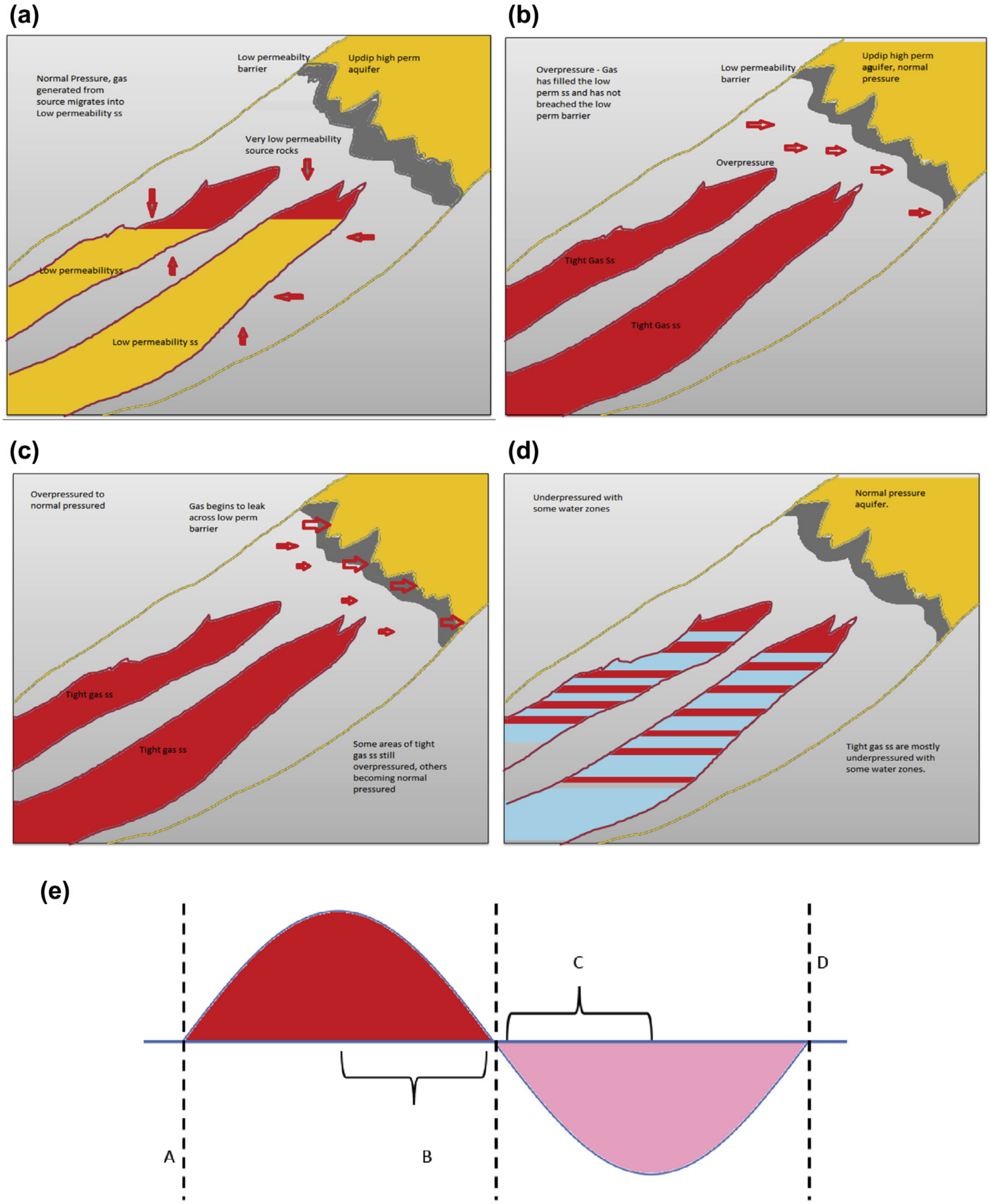

FIGURE 14.2

(a) Low permeability sands are charged by hydrocarbons produced by source shales. A very low permeability barrier prevents the hydrocarbons from escaping into the updip aquifer. Pressure varies from normal to

Moreover, the source rock should be subjected to heat transformation within the gas-generation window under burial history. Therefore, it is good practice to select exploration targets proximal to organically rich intervals (Coleman, 2008).

14.1.3.2 Abnormal Pressures

The productive intervals of a tight gas sandstone reservoir, in general, are abnormally pressured, either overpressured or underpressured (Meckel and Thomasson, 2008). The formation pressure depends on the structure, stratigraphy, and basin history. In general, when the source rock generates a large amount of gas in tight formations, gas cannot escape easily and causes overpressure in the system (Meckel and Thomasson, 2008). When some amount of the generated gas escapes from the updip margins of the overpressured area, an underpressured rim around the overpressured area may be generated. Measurements need to be acquired to characterize the pressure before development.

Burnie et al. (2008) discussed the mechanism for over and underpressure of tight gas sandstone reservoirs. Low permeability sandstones encased in shaly source rocks can be charged with gas. The pressure will build and the tight sandstones will be overpressured, but a low permeability barrier above them will contain the gas. Once a certain pressure threshold is reached, the gas will begin leaking through the low permeability barrier and escape updip. This will reduce the pressure to a normal and ultimately underpressure state. Figure 14.2 shows this pressure evolution, gas generation, and maturity model. Before the organic matter becomes mature, the pressure of the system is essentially normal. As the organic matters matures, i.e., during the active gas generation, the pressure builds up and the system becomes overpressured. In the postgeneration, the pressure of the system decreases and eventually becomes underpressured.

14.1.3.3 Stacking Patterns

Two basic types of tight gas sandstone reservoirs can be distinguished: stacked sandstones and blanket sandstones; they are related to the depositional environments. The stacked sandstones are often turbidites, deltas, or braided streams while blanket sandstones are usually extensive, laminated shallow-marine deposits. The stacked sandstones can have thousands of feet of 5–15 ft thick sand bodies of limited extent, while the blanket sandstones can be thin or thick, but typically thicker (20–30 ft) with greater areal extent. The stacked sandstones generally need to be drilled vertically or near vertically to

overpressured. In favorable areas, hydrocarbons can be produced. (b) Tight gas sands are fully charged and overpressured. Hydrocarbons with minor water are producible. (c) The pressure reaches a point where it breaches the overlying low permeability zone and hydrocarbons begin to leak through the barrier into the overlying aquifer. Pressure drops from over to underpressure. Hydrocarbons can be mostly produced, but water will begin to encroach. (d) Leakage has stopped and the sands are underpressured, and some hydrocarbons may be left in favorable areas along with producible water. (e) Pressure evolution model for tight gas reservoirs (pressure as a function of time; red (black in print versions) is overpressure, and pink (gray in print versions) is underpressure. A, normal pressure, hydrocarbon generation begins; B, overpressure, hydrocarbons contained; C, seal breached by overpressure, hydrocarbons migrate until pressure stabilizes; D, normal to underpressured, hydrocarbons contained.

Modified from Meckel and Thomasson (2008) and Burnie et al., 2008).

contact as many sandstone bodies as possible for better stimulation, while the laminated blanket sandstones need to be drilled horizontally to contact as much of the sandstone bodies as possible for better stimulation. Combinations of these types can also exist, along with conventional reservoir intervals. Examples of stacked sandstone reservoirs with high pressure include Pinedale (Webb et al., 2004; Ma et al., 2011), Jonah (Cluff and Cluff, 2004; Jennings and Ault, 2004), and Wamsutter (Barrett, 1994) fields, and examples of the stacked sandstones with moderate pressure include Williams Fork formation in the Piceance Basin (Hood, and Yurewicz, 2008) and Travis Peak formation in the East Texas Basin. The Frontier formation in the Green River basin and the Mancos B sandstones in the Piceance Basin are rather blanket sandstones (Finley, and O'Shea, 1985).

14.1.3.4 Reservoir Quality

Tight gas sandstones can range from mostly quartz to a variable mixture of quartz, feldspars, clays, carbonates, and pyrite. Matrix values can range from textbook sandstone values to very high or low values, so it is important to use actual rock data to determine the complexity of the reservoir. In some reservoirs, a single porosity calculation (density or sonic) may be adequate to get a useable interpretation, but in others a multimineral model with a variable number of clay and nonclay constituents may be needed. Average porosity for many known tight gas sandstones ranges between 7 and 10%, but lower or higher average porosities are also possible (Meckel and Thomasson, 2008). Average permeability often is in the order of 0.01 mD. Natural fractures may be important to producibility in tight gas sandstone reservoirs, but they may increase water production as well.

Based on the lithofacies characterization and petrophysical evaluation, completion technique and quality will drive the economic viability of each play. Reservoir quality is discussed in detail in the next chapter.

14.1.4 DRILLING, COMPLETION, AND DEVELOPMENT SCENARIOS

Because of the low permeability in tight gas sandstones, more wells are drilled to develop them compared with developing a conventional gas reservoir. A well life is typically longer as the initial high production rate may drop off fast to a plateau. Over the life time of a tight gas development, modest investments are made over a longer period than for developing a conventional gas reservoir (David and Stauble, 2013).

Typically, the stacked sandstone reservoirs are best drilled with vertical wells while the blanket sandstones are best drilled with horizontal wells. However, some stacked sand plays have many successful horizontal wells (Wei and Xu, 2015). In practice, understanding the spatial distribution of sand bodies, including their size and geometry, and using an integrated approach is critical in developing a tight gas sandstone reservoir. Pranata et al. (2014) presented an example of achieving high production rate using an integrated reservoir characterization approach and the dual-lateral horizontal technology without using the hydraulic fracturing.

Drilling challenges in the tight sandstones include lost circulation due to natural fractures or low pressure, sloughing of shale layers, formation damage, mud invasion, and drilling bit abrasion (Pilisi et al., 2010). A number of drilling methods are available for developing tight gas sandstone reservoirs, including conventional drilling, casing drilling, coiled tubing drilling, underbalanced drilling, overbalanced drilling, and managed pressure drilling, each of which have advantages and limitations (Table 14.1, also see Pilisi et al., 2010).

Table 14.1 Comparing Different Drilling Methods

Drilling Method	Conventional	Casing	Coiled Tubing	Overbalanced	Underbalanced	Managed Pressure
Drilling problem: lost circulation, stuck pipe, etc.	May increase	Lower	No effect	May be high	Lower	Much lower
Reduce formation damage	No	Little	No	No	Yes	Yes
Kick detection				Yes	Yes	Yes
Equipment complexity	Low	Medium	Medium	Low	High	High
Rate Of Penetration (ROP) improvement	No	Little	Yes (smaller diameter)	No	Yes	Yes

Modified from Pilisi et al. (2010).

For stacked sandstone reservoirs, designing the hydraulic fracture treatment should be based on the formation evaluation, especially the lithofacies layering geometry as the completion is based on the producing zones that are separated by vertical flow barrier layers (Holditch, 2006). The number of stages, for example, can be determined based on the stacking pattern of the geometry of sand bodies and shaly barriers. Depending on the thickness of the sand and shale layers and formation in situ stress profile, a single fracture treatment can be sometimes used to stimulate multiple layers, the well can be completed and stimulated with a single stage, and gas will be produced by commingling the different layers. On the other hand, when a thick shale barrier separates two productive layers, multiple hydraulic fractures should be created, especially when the in situ stress contrast is high.

One important decision to make in completing a tight gas sandstone reservoir is to select a diversion method (Table 14.2, also see Holditch and Bogatchev, 2008; Wei et al., 2009). A number of diversion techniques are available and each of them has certain advantages, disadvantages, and limitations (Wei et al., 2010). The selection of diversion technique should be based on the following parameters:

- number of layers,
- depth of each layer,
- net pay thickness in each layer,
- effective porosity in each layer,
- water saturation in each layer,
- drainage area for each layer,
- pressure and temperature in each layer, and
- gas gravity.

Table 14.2 Issues and Decisions in Various Stages of Developing Tight Gas Sandstone Reservoirs

Evaluation	Drilling	Completion	Production
Basin analysis and regional geology	Method selection	Stage count	Gas flow rate
Stratigraphy/structural analysis	Lost circulation	Diversion technique	Water production
Seismic interpretation and attribute analysis	Stuck pipe	Perforation design	Artificial lift
Formation evaluation with well logs and core data	Formation damage	Fluid selection	Tubing design
3D reservoir model	Sloughing, kicks	Proppant selection	Casing diameter

14.2 LITHOFACIES AND ROCK TYPING

As tight gas sandstone reservoirs reside in siliciclastic formations, their lithofacies typically include sandstone, siltstone, and shale based on grain size; alternatively, they can be divided into sand, sandy shale, shaly sand, and shale. Modeling lithofacies is generally sufficient for characterizing tight gas sandstone reservoirs although special care may be needed to assess the impact of minerals on the logs (Ma et al., 2011, 2014a). For example, based on depositional characteristics, fluvial deposits often include sand-dominant channel facies, shale-dominant floodplain, and a mixture of sand and shale in the crevasse and splay facies. Rushing et al. (2008) summarized a list of rock type definitions from 26 studies on sandstone reservoirs. There is much debate regarding definition of rock types, depending on the classification scheme used: depositional, petrographic, log-based, or hydraulic. Depositional rock types are defined in the context of the large-scale geological framework and represent the rock properties at deposition, and they are generally termed depositional facies, such as channel, overbank, crevasse, and splay. Petrographic rock types are based on small-scale, microscopic rock properties, typically defined with the aid of various imaging tools (Rushing et al., 2008). Log-based rock types are typically called electrofacies, and they represent the signature of wireline logs (Wolff and Pelissier-Combescure, 1982). Hydraulic rock types are mainly based on the rock flow properties, such as flow zone indicator or FZI (Amaefule et al., 1993). Because the subsurface formations are subject to multiple geological processes, including deposition, erosion, redeposition, compaction, and diagenesis, these definitions of rock types are generally very different; it is often impossible to establish a consistent match between two different definitions. The three most commonly used definitions include lithofacies that have a connotation of depositional facies and lithology, electrofacies that are defined using logs, but not necessarily calibrated to geology, and rock types based on FZI or other petrophysical and/or engineering criteria. Lithofacies are closely related to geology because lithology represents compositional mineral content and geologic facies are highly related to depositional environments. Thus the calibration of electrofacies to lithofacies can relate the logs to geology more closely, but it is not always straightforward. The advantage of using lithofacies is that they can be modeled using geologic propensity analysis so that the 3D lithofacies model is consistent with the conceptual depositional model based on sedimentary and sequence-stratigraphic analyses (Ma, 2009). This is especially important when data are limited.

We discuss methods of electrofacies and lithofacies classification with an emphasis on lithofacies. Electrofacies are clusters defined from wireline logs, and as such, they may or may not be lithofacies before calibration to geologic interpretations. Moreover, smaller-scale electrofacies can also be modeled within a lithofacies in a hierarchical order. This can be carried out using a cascaded methodology (Ma, 2011).

14.2.1 LITHOFACIES IN TIGHT GAS SANDSTONES AND WIRELINE LOGS

Wireline logs provide basic data sources for evaluating petrophysical properties as they measure some characteristics of the rock formations. Histograms of wireline logs can be used to assess the possible separations of various lithofacies (Ma et al., 2014a). The most striking characteristic of a mixture of multiple lithofacies is the multimodality in the histograms of logs. This also explains why logs rarely show a normal distribution, but rather they are characterized by either a multimodal histogram or a skewed long-tail in the histogram. Depositional or lithological facies are often a dominant factor that causes the nonnormality, including multimodality and skewness, in the histogram of a wireline log.

More specifically, logs in a tight sandstone formation often show bimodality (sometimes more than bimodal) in their histograms (Fig. 14.3), but notice that bimodality may conceal the existence of more than two mixtures of lithofacies. For instance, the GR (Gamma Ray) histogram (Fig. 14.3(a)) cannot be decomposed into two quasinormal histograms, but rather into three quasinormal histograms (Ma et al., 2014b). This is because the GR log conveys a three-lithofacies mixture. Resistivity and porosity logs in Fig. 14.3 also reflect the mixtures of three lithofacies. Typically, many wireline logs carry information about the lithofacies, but none of them is individually capable of accurately discriminating them. Two or more logs are typically needed to accurately separate the individual lithofacies because of the overlaps of lithofacies mixtures on the logs.

A basic exploratory tool for multivariate analysis is the correlation or correlation matrix that includes correlation coefficients between any two variables of concern. Graphic displays, such as cross plots, and two-dimensional (2D) histograms, often enable an insightful analysis of the relationship between two variables and the characteristics of the lithofacies mixtures. For example, the 2D histogram of the GR and logarithm of the resistivity (Fig. 14.3(d)) shows three modes while the monovariate histograms of GR and resistivity show only two modes (Fig. 14.3(a)–(c)). Similarly, the 2D histogram of porosity and GR reveals three modes, albeit discreetly (Fig. 14.3(e)). In theory, a multidimensional joint probability histogram reveals even more clearly the data structures of a mixture, but there is no effective way to display it graphically; a 2D histogram matrix can be used to gain insights into multivariate relationships of numerous wireline logs (Ma et al., 2014b).

14.2.2 LITHOFACIES CLASSIFICATION USING WIRELINE LOGS IN TIGHT GAS SANDSTONE FORMATIONS

The importance of classification of lithofacies for tight gas reservoirs lies in identifying potential gas zones using wireline logs because recoverable gas resides mostly in sand-dominated lithofacies, and marginally in silty lithofacies.

14.2.2.1 Problem of Cutoff Methods

The two modes in the histogram of individual logs (Fig. 14.3) often suggest more than two lithofacies. In the well-log GR histogram (Fig. 14.3(a)), two modes are pronounced with the smaller mode at

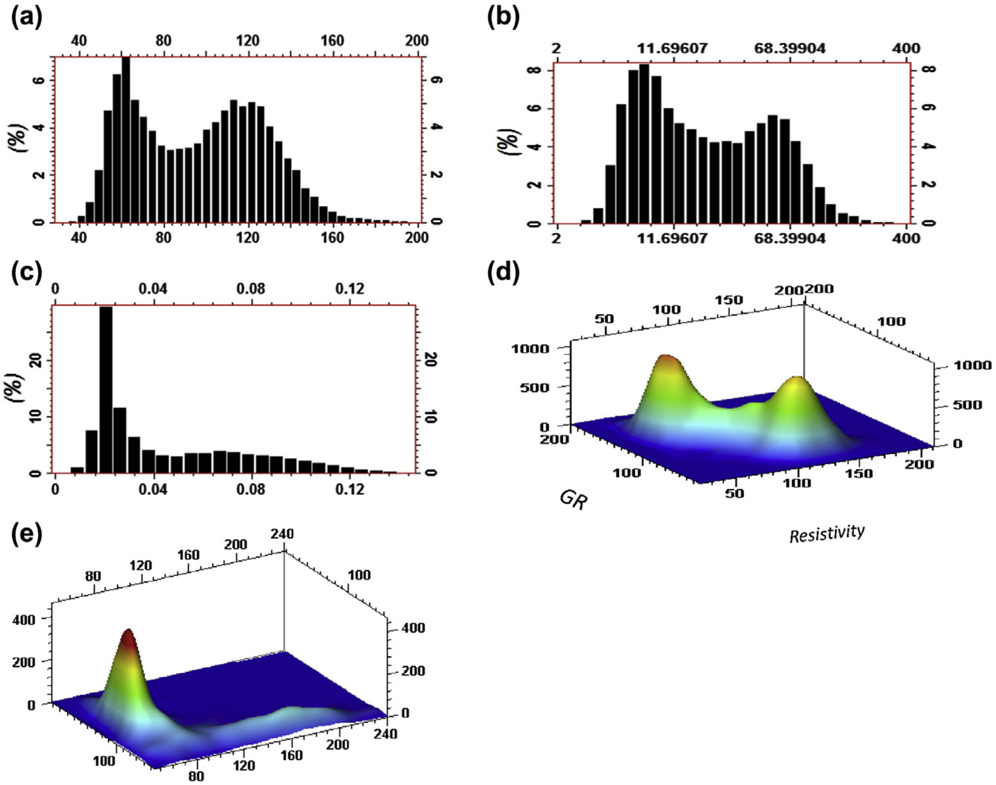

FIGURE 14.3

Histogram examples of wireline logs in tight gas sandstones. (a) GR; (b) logarithmic resistivity; (c) porosity; (d) 2D histogram of GR-logarithmic resistivity; (e) 2D histograms of porosity-GR (porosity ranges between 0 and 15%, and was rescaled to between 0 and 250 for display purpose).

approximately 60 API and the larger mode at approximately 120 API. Traditionally, a cutoff was used to generate the sandy lithofacies from low GR values, silty lithofacies from moderate GR values, and the shaly lithofacies from high GR values, such as shown by the example in Fig. 14.4(a). However, these three lithofacies exhibit significant overlaps in the GR distributions based on core data (Fig. 14.4(b)). Only the smallest and largest GR values (less than 60 API or more than 120 API) do not have significant overlaps of the three lithofacies, but GR values between 60 and 120 API are a mixture of samples from all the three lithofacies (Ma et al., 2011, 2014a).

Therefore, the method of applying cutoffs to the GR log is not optimal as it results in the three lithofacies at different GR bands. Using GR alone misclassifies many samples into the wrong lithofacies. Many sandy and shaly samples with GR values between 85 and 95 API are incorrectly classified as siltstones. Many siltstone samples with GR values below 80 API or above 100 API are incorrectly classified as either sand or shale samples. As sandy lithofacies are hydrocarbon-bearing and shale lithofacies are nonreservoir rocks, misclassification of shale lithofacies into sand lithofacies leads to false positives, and the converse leads to false negatives. When two or more logs are used, the

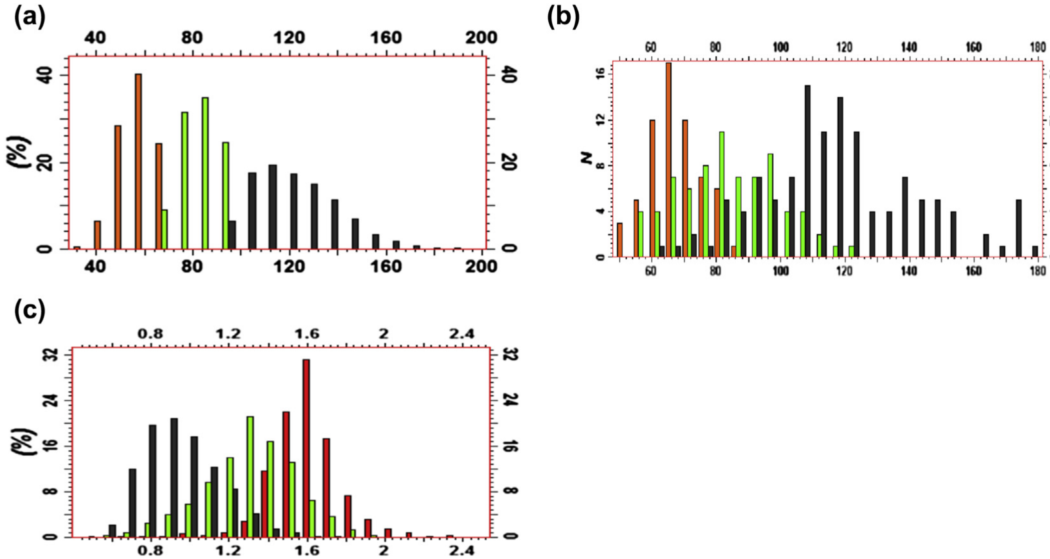

FIGURE 14.4

(a) Decomposition of the histogram in Fig. 14.3(b) into three histograms based on the GR cutoffs. Color code: orange (dark gray in print versions), channel facies; green (gray in print versions), crevasse-splay; and black, overbank. (b) GR histograms by lithofacies from core data from one well in the Greater Green River basin. (c) Resistivity histograms for the three lithofacies clustered using GR cutoffs. Note that the histograms of the different lithofacies on the same plots in (b) and (c) are not normalized together, but each histogram is normalized by itself. Therefore, the display does not show the relative proportion of each histogram over the total population.

cutoff method uses a gated logic for lithofacies classification, but the gated logic is not optimal as it causes many boundary effects. A different approach is needed to more accurately discriminate the overlapped GR or other log samples into different lithofacies.

14.2.2.2 Lithofacies Classification from Mixture Decomposition of Wireline Logs

Although the histograms of many logs show only two modes, they cannot be modeled by two normal or quasinormal distributions, but some of them can be aptly fitted into three quasinormal distributions. This is because the frequency distribution of an individual log signature by the silty lithofacies often overlaps completely with the log signature of the sandy and shaly lithofacies, and their modes are hidden in the histogram. The main idea of lithofacies mixture decomposition lies in use of multiple logs to separate the overlaps in individual logs.

Resistivity is often a good discriminator for classification of the lithofacies when no aquifer is present, which is quite common for tight gas sandstone reservoirs (Law et al., 1986, 2002; Naik, 2003; Aguilera and Harding, 2008). Whereas shaly lithofacies typically have lower resistivity responses because of the absence of gas and more bounded water, sandstones exhibit higher resistivity as a result of bearing hydrocarbon and lower bounded water content. The GR and resistivity logs are generally correlated negatively; their correlation is −0.821 using the logarithm of the resistivity

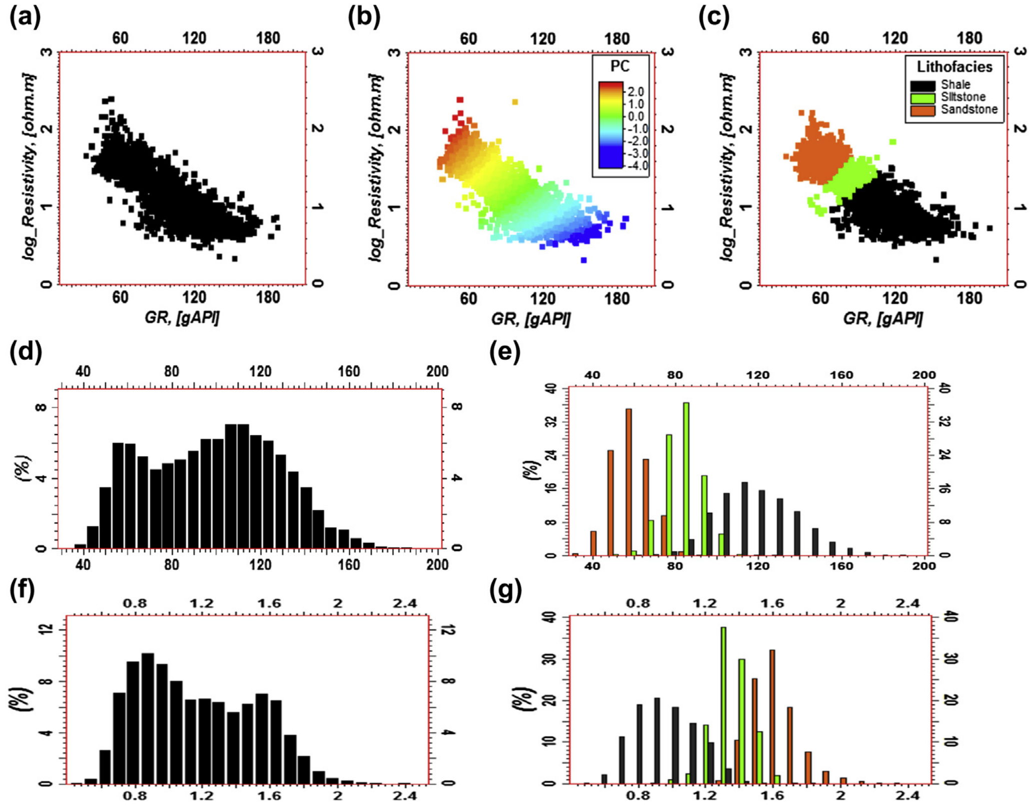

FIGURE 14.5

(a) GR–resistivity (logarithm) cross plot. (b) GR–resistivity (logarithm) cross plot overlain with the first PC of PCA of the two logs. (c) GR–resistivity (logarithm) cross plot overlain with the three clustered lithofacies. (d) GR histogram. (e) GR histograms for three clustered lithofacies. (f) Logarithmic resistivity histogram. (g) Logarithmic resistivity histogram for the three clustered lithofacies. Orange (gray in print versions) represents the sandstones; black, shale; and green (light gray in print versions), siltstones. For (f) and (g), see the note in Fig. 14.2.

in the example (Fig. 14.5). The resistivity log also shows two modes similar to the GR histogram, but the larger mode corresponds to smaller resistivity values, and the smaller mode corresponds to large resistivity values. This is because the two logs are negatively correlated and there is significantly more shale than sand in the formation.

Principal component analysis, or PCA, (a tutorial is found in the appendix of Chapter 7) can be used to combine the two or more logs for classification of these lithofacies. Here, we show examples of classifying the three lithofacies using PCA over two logs: GR and resistivity. The three lithofacies clustered using PC1 are shown in Fig. 14.5. Notice the three component histograms are similar to the experimental histograms based on the core data except that the core data histograms are less normal because of the limited data. Similarly, the three lithofacies overlap between 9 and 40 Ω on the resistivity; overlapping resistivity values between the three lithofacies implies that these lithofacies cannot be correctly classified using the resistivity log alone, but the resistivity histogram was decomposed into three component histograms in the classification of the three lithofacies (Fig. 14.5(e)). Statistically, this can be considered as a mixture decomposition that separates the component histograms from the original histogram (Ma et al., 2014b). Although this example uses only two logs, three or more logs can be used in the same workflow as PCA is very effective to handle multiple input variables for classification of the lithofacies. Readers can find a lithofacies classification example using three logs in Ma et al. (2014a).

Moreover, principal components can be rotated to emphasize importance of one log versus the others (Ma, 2011). Three or more logs can be used for classification as well using PCA (Ma, 2011; Ma et al., 2014b).

14.2.2.3 Determining Proportions of Lithofacies in Classification

The determination of the proportion of each lithofacies in classification is important because it impacts the assessment of the overall reservoir quality of the field. In tight gas sandstone reservoirs, a higher proportion of sandy lithofacies from the clustering than the true proportion will cause an optimistic view of the reservoir, and a higher proportion of shaly lithofacies will lead to a pessimistic view. Ideally, lithofacies data from core are abundant and representative without sampling bias, and then they can be used as a reference for the proportions. Unfortunately, core lithofacies are generally limited and statistically are rarely representative. Purely automatic methods, including unsupervised artificial neural network (ANN) and statistical techniques, are not robust enough to generate accurate proportions of lithofacies. In sandstone formations, ANN typically yields more siltstone in classification because automatic methods have a tendency to make similar proportions for all the clusters, unless the clusters are highly distinct. Moreover, siltstone typically has intermediate values for many logs, such as GR, resistivity and effective porosity, but the intermediate values do not always correspond to siltstone. The relatively abundant overlapping intermediate values easily cause an over classification of siltstone than its true proportion for most automatic methods.

PCA has an advantage over ANN as it enables determining the proportion of each clustered lithofacies using the cumulative histogram of a selected PC or rotated PC. As ANN makes the lithofacies classification purely based on the data structures, it does not incorporate the significance of each input log. For example, ANN clustering based on GR and resistivity in the previous example gives unrealistic clusters, as shown in Fig. 14.6(a), in which some samples with lower GR and higher resistivity are classified to be siltstone while higher GR and lower resistivity samples are classified as sandstone. It is possible to overcome the problem by combining PCA and ANN, i.e., ANN using only the first PC, such as shown in Fig. 14.6(b).

The method presented here includes: (1) generating lithofacies by applying cutoffs on some selected but representative principal component(s), and (2) using the generated data as training data for applying the supervised ANN. In classifications using PCA, the number of quasinormal distributions decomposed from the initial histogram can be used as an initial estimate of the number of lithofacies that have similar petrophysical characteristics. The proportion of each lithofacies is inferred from the decomposition of the histogram. The ratio of the cumulative frequency of each of the three component histograms to the cumulative frequency of the composite GR histogram is the proportion of the

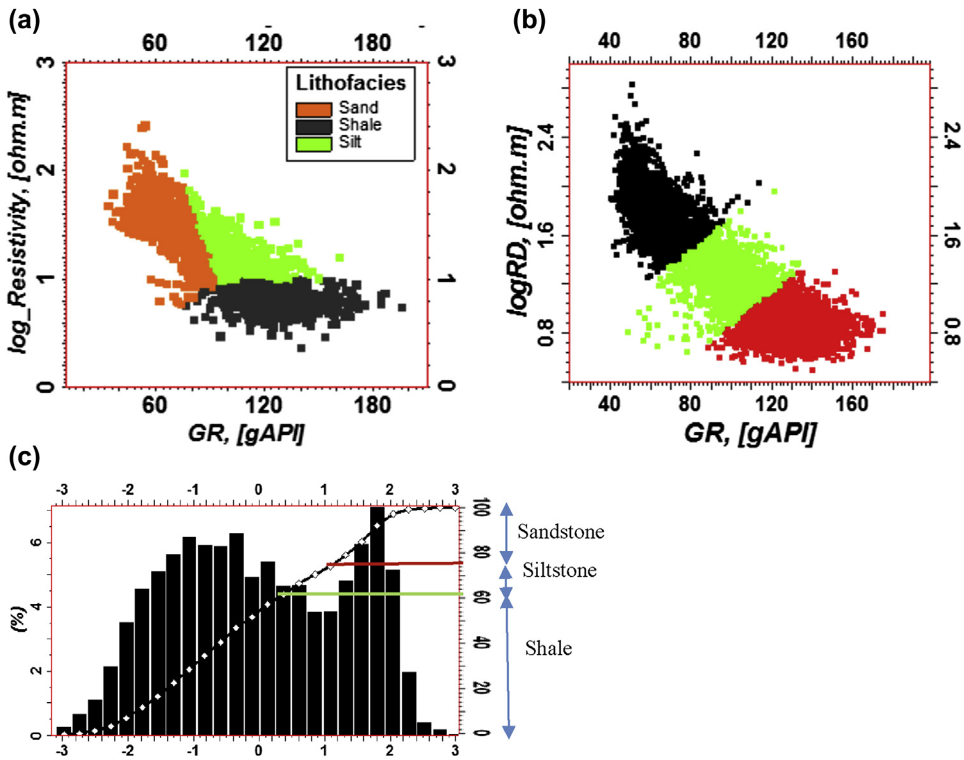

FIGURE 14.6

(a) GR-resistivity (logarithm) cross plot, overlaid with the lithofacies clustered using ANN. (b) GR–RD (Gamma ray-resistivity) cross plot overlain with the lithofacies clustered by ANN using PC1. (c) Illustrating the cutoff method and the proportions of the three clustered lithofacies using cumulative histogram of a PC (histogram is displayed in the background).

corresponding lithofacies. When one component, such as PC1, is used for clustering, it is straightforward to find the cutoff values that give a predetermined proportion for each lithofacies, as illustrated in Fig. 14.6(c). In this example, the clustered shale represents 60.3%, siltstone 13.9%, and sandstone 25.8%. In comparison, the clustering by ANN (Fig. 14.4(a)) gave 37.4% shale, 35.6% siltstone, and 26.9% sandstone. The latter proportions are highly inconsistent with the outcrop observation and other analogs.

This method of using the cumulative histogram to define the proportions of the lithofacies clusters is very general; it can be used with any variable or component. For example, it can be used even for the cutoff method with a single wireline log, but we have already shown the limitation of using a single log. Notice also that the example in Fig. 14.6(c) is an original PC, but this component can be a rotated component that represents information from a number of the original PCs.

14.2.3 IMPACT OF LITHOFACIES CLASSIFICATION ON STACKING PATTERNS AND DEPOSITIONAL INTERPRETATION

Different methods for lithofacies classification have a significant impact on the interpretation of the deposition, net-to-gross (NTG), and stacking patterns. Typically, the cutoff methods generate too much intermediate-quality rocks, such as siltstone or crevasse–splay facies. Figure 14.7(a) compares the lithofacies vertical sequences by the cutoff method, PCA, and ANN for the example discussed above (Figs 14.4 and 14.5) for one well. The GR cutoff method generated much more siltstone, and less sandstone than the PCA. On the other hand, ANN generated much more sandstone, and less shale than the PCA. This is also true for all the wells in the model area. The vertical proportion profiles (VPPs) of the lithofacies generated by the three methods are also compared (Fig. 14.7).

The three lithofacies proportions are 55.3% shale, 22.3% siltstone, and 22.4% sandstone for the GR cutoff method; 60.3% for shale, 13.9% for siltstone, and 25.8% for sandstone for the PCA; 35.6% shale, 26.9% siltstone, and 37.4% sandstone for ANN. For each VPP, each stratigraphic unit had different fractions of those lithofacies. Relative fractions of the three facies can differ from layer to layer. Lithofacies VPP represents an "average" stacking pattern and can be used to analyze and model vertical sequence succession of depositional facies (Ma et al., 2009).

Variogram of lithofacies often shows a certain so-called "hole" effect, which reflects cyclicity of the lithofacies (Jones and Ma, 2001). For blanket sandstones, cyclicity is mainly in the vertical direction as the lateral sandstone layers are generally extensive. For stacked, lenticular sandstones, cyclicity can appear both vertically and laterally, but generally stronger in the vertical direction because of the lithofacies depositional sequence. The vertical cyclicity in the lithofacies is highly related to the stacking pattern and vertical proportion profiles.

14.3 THREE-DIMENSIONAL MODELING OF LITHOFACIES IN TIGHT SANDSTONE FORMATIONS

Populating a 3D lithofacies model using the lithofacies data at the wells commonly requires upscaling the lithofacies samples into the 3D grid because well logs typically have a half-foot sampling rate and 3D grid cells have a larger size. All known methods for upscaling a categorical variable are statistically biased as they use the "winner-take-all" approach (Ma, 2009). The method of most-abundant-value, which is the most reasonable and most common one, tends to favor the major lithofacies while reducing minor lithofacies. This problem can be bypassed if the lithofacies data at wells are predicted from wireline logs. Instead of creating lithofacies at the well-log scale, the continuous variables used for the lithofacies prediction can be upscaled into the 3D grid with an unbiased method, and then they can be used for lithofacies classification directly in the grid-cell scale (Ma et al., 2011). Detail of this workflow is beyond the scope here, we assume availability of upscaled lithofacies data at wells before the 3D modeling.

For blanket sandstone reservoirs, stratigraphic correlation is relatively simpler when enough wells are available, and the lithofacies model may be constructed in a relatively straightforward way, for example using sequential indicator simulation (SIS) with a large horizontal variogram range because of the large lateral continuity. Here, we compare four common methods of modeling lithofacies for a stacked, fluvial sandstone reservoir. These four methods for modeling categorical variables are presented in the Appendix. Among these techniques, object-based modeling (OBM) generally is more

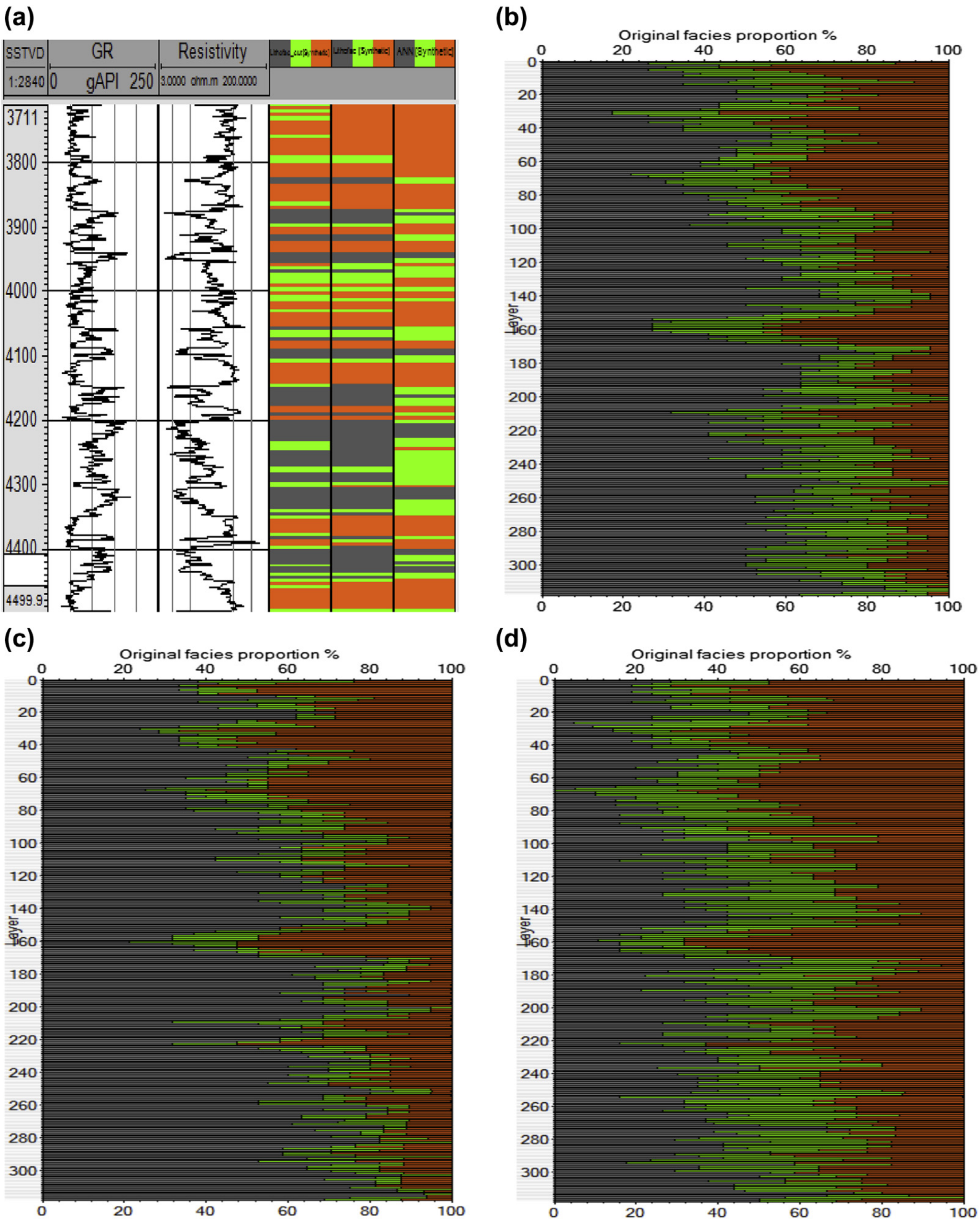

FIGURE 14.7

(a) Well section showing GR (Track 1), resistivity (Track 2), zonation of the clustered lithofacies by the GR cutoff (Track 3), zonation of lithofacies by the PCA using both GR and resistivity (Track 4), and zonation of lithofacies generated by ANN (Track 5). (b) Vertical profile of the clustered lithofacies by GR cutoffs using all the 20 wells in the model area. (c) Vertical profile of the clustered lithofacies by PCA using all the 20 wells in the model area. (d) Vertical profile of the clustered lithofacies by ANN using all the 20 wells in the model area. Orange (gray in print versions) represents sandy lithofacies, yellow (light gray in print versions) the silty lithofacies, and black the shaly lithofacies (Greater Green River basin).

suitable for clear shape definitions of geologic bodies, such as channels and bars. The truncated Gaussian method is more suitable when the order of the facies is clearly definable. SIS is one of the most commonly used geostatistical methods to model lithofacies because of its capabilities in integrating various data. In particular, lithofacies probability maps or volumes can be integrated more easily in the SIS model than in the other modeling methods to constrain the positioning of the lithofacies bodies. The model by the method with user-defined objects generally has spatial characteristics between the models generated by OBM and SIS.

Figure 14.8(a) shows a relatively small area with 20 wells, wherein the lithofacies data were obtained by PCA classification using GR and resistivity (as discussed earlier). Without other information,

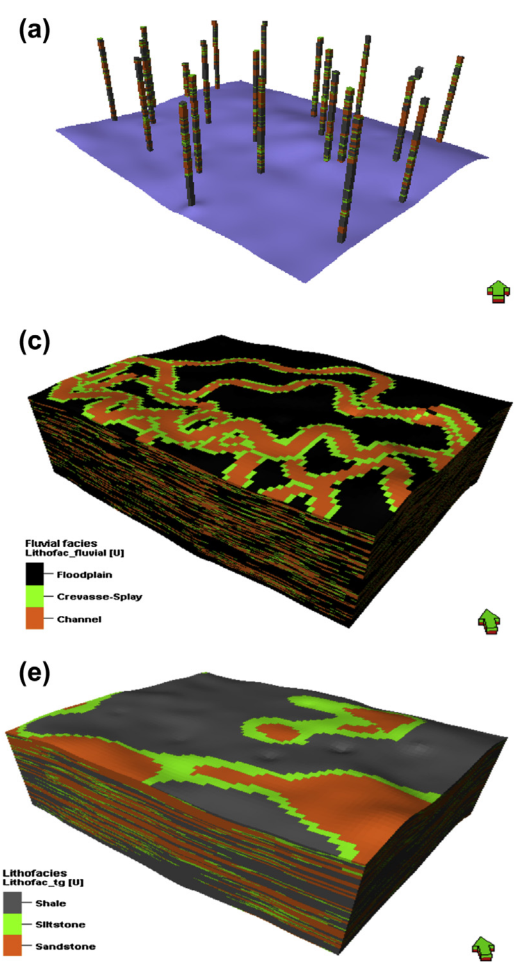

FIGURE 14.8

(a) Lithofacies data at 20 wells, classified by PCA. (b) 3D lithofacies model constructed by SIS honoring the data in (a). (c) 3D lithofacies model constructed using fluvial OBM. (d) 3D lithofacies model constructed using user-defined objects (ellipses with rounded base). (e) 3D lithofacies model constructed using truncated Gaussian simulation. Notice the halos of the siltstone (intermediate lithofacies) around the sand lithofacies.

the knowledge of fluvial system as the depositional environment by itself cannot always determine the best method for populating the lithofacies in the 3D model. Given the fluvial example with 20 wells, four 3D lithofacies models using different methods are shown in Fig. 14.8(b)–(e). As no probability is used for conditioning, the SIS model (Fig. 14.8(b)) is driven by the indictor variogram and data from the wells. As a result of the scarcity of the data, the facies objects are often distributed randomly, especially in the areas of no control points. The model using fluvial OBM method (Fig. 14.8(c)) mimics the fluvial depositional characteristics, including meandering of the channels, and amalgamation and cutting between the channels. Figure 14.8(d) shows a 3D lithofacies model constructed using ellipses with rounded base. The lithofacies model using this type of defined objects often has characteristics between fluvial OBM and SIS models.

Notice the halos of siltstone (intermediate lithofacies) around the sand lithofacies in the truncated Gaussian model (Fig. 14.8(e)). This is because the truncated Gaussian simulation imposes a sequence of transitions between different lithofacies, which can be a drawback in some situations. This problem can be mitigated by an enhanced method, termed truncated pluri-Gaussian simulation (Galli et al., 1994; Hu et al., 2001).

One limitation of the fluvial OBM technique is that the geometry of crevasse–splay facies may not be modeled realistically because many modeled crevasses or splays do not form as small fans breaking off from channels. For sedimentary process modeling, this would be a serious problem. In reservoir modeling, however, facies are highly linked with the petrophysical properties that directly determine the hydrocarbon pore volume and fluid flows. Using facies to indicate the reservoir quality of rocks is an important consideration.

In practice, each stratigraphic unit typically has different facies proportions and associations. In the case of fluvial channel deposition, the channel characteristics differ from one stratigraphic package to another, including orientation, width, and thickness. Uncertainties in channel characteristics, including orientations, sinuosity, width, and thickness can be expressed as probabilistic distributions of a triangle, uniform, Gaussian function, or truncated Gaussian function. Lithofacies stacking patterns are related to the facies fraction for each stratigraphic zone in the model. Vertical proportion curves in the facies vertical profile, object dimensions, and facies data at the wells can be honored, at least to certain extent. In the discussed example, more continuity occurs in the channels along the main depositional direction (north-west to south-east). Channel sinuosity and lateral and vertical amalgamations of channel and crevasses facies are evident (Fig. 14.8). Well correlation shows good sand continuity, especially from the north-west to south-east, which is the preferential orientation of the channels.

14.4 CONCLUSION

A variety of depositional environments exist for tight gas sandstone reservoirs. A realistic lithofacies model is important as it impacts the spatial distribution of the main reservoir properties. A good lithofacies model should realistically capture the important reservoir heterogeneity. Generally, there is a lack of core lithofacies data for field-wide reservoir analysis, and lithofacies are obtained from wireline logs. We combine the classical petrophysical analysis with statistical methods and neural networks for lithofacies clustering. These methods enable classifying lithofacies by integrating geological and petrophysical interpretation.

All the categorical-modeling techniques can be hierarchized in two or more levels for multilevel facies modeling. For example, facies may be first modeled using fluvial OBM or truncated Gaussian method, and then modeled again using SIS based on the model already constructed by OBM or truncated Gaussian method. This is because OBM and truncated Gaussian methods generally produce larger facies objects in the model, and SIS can be further used to model small-scale heterogeneities. In fact, the workflow of modeling lithofacies by SIS following a truncated Gaussian modeling or OBM has been applied to a number of hydrocarbon field-development case studies, including carbonate ramps and shallow-marine depositional environments. An example of constructing a facies model using OBM based on the model constructed by SIS can be found in Cao et al. (2014), in which a facies model of sand-shale was first built using SIS with facies probability maps. Then a fluvial OBM method was used to generate channels with splays.

Because of the complexity of geological deposits, modeling lithofacies is simultaneously indeterministic and causal. In a large-scale model where depositional trends are geologically definable, lithofacies probability maps or cubes can be constructed while incorporating the depositional trends (Ma, 2009); these probability maps or cubes can be used to constrain the 3D lithofacies model, along with the data at wells.

ACKNOWLEDGMENT

The authors thank Schlumberger Ltd for permission to publish this work. They also thank Dr Shujie Liu and Mi Zhou for reviewing the manuscript.

REFERENCES

Amaefule, J.O., Altunbay, M., Tiab, D., Kersey, D.G., Keelan, D.K., 1993. Enhanced reservoir description: using core and log data to identify hydraulic (flow) units and predict permeability in uncored intervals/wells: SPE 26436. In: 68th Annual Technology Conference and Exhibition Houston, Texas.

Aguilera, R., Harding, T.G., 2008. State-of-the-art tight gas sands characterization and production technology. Journal of Canadian Petroleum Technology 47 (12).

Barrett, F.J., 1994. Exploration and development of almond tight gas sands along the Wamsutter/Creston Arch, Wasahakie-red Desert basins, Southwest Wyoming. AAPG Search and Discovery. Article #90986, presented at AAPG Annual Convention, Denver, Colorado, June 12–15, 1994.

Burnie, S.W., Maini, B., Palmer, B.R., Rakhit, K., 2008. Experimental and empirical observations supporting a capillary model involving gas generation, migration, and seal leakage for the origin and occurrence of regional gasifers. In: Cumella, S.P., Shanley, K.W., Camp, W.K. (Eds.), Understanding, Exploring, and Developing Tight Gas Sands, 2005 Vail Hedberg Conference, AAPG Hedberg Series, vol. 3, pp. 29–48.

Camp, W.K., 2008. Basin-centered gas or subtle conventional traps? In: Cumella, S.P., Shanley, K.W., Camp, W.K. (Eds.), Understanding, Exploring, and Developing Tight Gas Sands, 2005 Vail Hedberg Conference, AAPG Hedberg Series, vol. 3, pp. 49–61.

Cao, R., Ma, Y.Z., Gomez, E., 2014. Geostatistical applications in petroleum reservoir modeling. Southern African Institute of Mining and Metallurgy 114, 625–629.

Clement, R., et al., 1990. A computer program for evaluation of fluvial reservoirs. North Sea Oil and Gas Reservoirs-II.

Cluff, S.G., Cluff, R.M., 2004. Petrophysics of the Lance Sandstone Reservoirs in Jonah Field, Sublette County, Wyoming, in AAPG Studies in Geology #52, Jonah Field: Case Study of a Tight-Gas Fluvial Reservoir pp. 215–241.

Coleman, J.L., 2008. Tight gas sandstone reservoirs: 25 years of searching for “The Answer”. In: Cumella, S.P., Shanley, K.W., Camp, W.K. (Eds.), Understanding, Exploring, and Developing Tight gas Sands, AAPG Hedberg Series, vol. 3, pp. 221–250. Tulsa, OK.

David, F., Stauble, M., 2013. Developing a sustainable unconventional business in China. In: SPE Paper 167051, Presented at the SPE Unconventional Resources Conference and Exhibition-Asia Pacific, Brisbana, Australia, November 11–13, 2013.

Deutsch, C.V., Journel, A.G., 1991. Geostatistical Software Library and User's Guide. Oxford Univ. Press, 340 p.

Finley, R.J., O'Shea, P.A., 1985. Geologic and engineering analysis of blanket-geometry tight gas sandstones. In: SPE-Doe Joint Symposium on Low Permeability Gas Reservoirs, Denver CO, March 13–16, 1985.

Galli, A., Beucher, H., Le Loc'h, G., Doligez, B., 1994. The pros and cons of the truncated Gaussian method. In Geostatistical Simulation. Quantitative Geology and Geostatistics 7, 217–233.

Holden, L., et al., 1997. Modeling of fluvial reservoirs with object models. In: AAPG Computer Applications in Geology, vol. 3.

Holditch, S.A., 2006a. Tight gas sands. Journal of Petroleum Technology (June) 86–93.

Holditch, S.A., 2006b. Optimal Simulation Treatments in Tight Gas Sands. SPE 96104.

Holditch, S.A., Bogatchev, K.Y., 2008. Developing Tight Gas Sand Adviser for Completion and Stimulation in Tight Gas Sand Reservoirs Worldwide. Paper SPE 114195, presented at the CIPC/SPE Gas Technology Symposium 2008 Joint Conference, Calgary Alberta, Canada, 16–19, June.

Hood, K.C., Yurewicz, D.A., 2008. In: Assessing the Mesaverde Basin-Centered Gas Play, Piceance Basin, Colorado. AAPG Hedberg Series, vol. 3, pp. 87–104. Tulsa, OK.

Hu, L.Y., Le Ravalec, M., Blanc, G., 2001. Gradual deformation and iterative calibration of truncated Gaussian simulations. Petroleum Geosciences 7, S25–S30.

Jennings, J.L., Ault, B.P., 2004. Jonah Field Completions: An Integrated Approach to Stimulation Optimization with an Enhanced Economic Value, in AAPG Studies in Geology #52, Jonah Field: Case Study of a Tight-gas Fluvial Reservoir, pp. 269–279.

Jones, T.A., Ma, Y.Z., 2001. Geologic characteristics of hole-effect variograms calculated from lithology-indicator variables. Mathematical Geology 33 (5), 615–629.

Journel, 1983. Nonparametric estimation of spatial distribution. Mathematical Geology 15 (3), 445–468.

Kazemi, H., October 1982. Low-permeability gas sands. Journal of Petroleum Technology.

Kennedy, R.L., Knecht, W.N., Georgi, D.T., 2012. Comparison and contrasts of shale gas and tight gas developments, North American experience and trends. In: SPE Paper 160855, Presented at the SPE Saudi Arabia Section Technical and Exhibition, Al-khobar, Saudi Arabia, 8–11 April.

Law, B.E., 1984. In: Law, B.E. (Ed.), Structure and Stratigraphy of the Pinedale Anticline, Wyoming, USGS Open-File 84–753.

Law, et al., 1986. Geologic Characterization of Low Permeability Gas Reservoirs in Selected Wells, Greater Green River Basin, Wyoming, Colorado, and Utah, AAPG SG 24, Geology of Tight Gas Reservoirs, pp. 253–269.

Law, B.E., Spencer, C.W., 1989. Geology of Tight Gas Reservoirs in Pinedale Anticline Area, Wyoming, and Multiwell Experiment Site, Colorado. In: US Geologic Survey Bulletin 1886.

Law, B.E., 2002. Basin-centered gas systems. AAPG Bulletin 86 (11), 1891–1919.

Ma, Y.Z., 2009. Propensity and probability in depositional facies analysis and modeling. Mathematical Geosciences 41, 737–760. http://dx.doi.org/10.1007/s11004-009-9239-z.

Ma, Y.Z., 2011. Lithofacies clustering using principal component analysis and neural network. Mathematical Geosciences 43, 401–419.

Ma, Y.Z., et al., 2014a. Identifying hydrocarbon zones in unconventional formations by discerning Simpson's paradox. Paper SPE 169496 presented at the SPE Western and Rocky Regional Conference, April, 2014.

Ma, Y.Z., Wang, H., Sitchler, J., et al., 2014b. Mixture decomposition and lithofacies clustering using wireline logs. Journal of Applied Geophysics 102, 10–20. http://dx.doi.org/10.1016/j.jappgeo.2013.12.011.

Ma, Y.Z., Gomez, E., Young, T.L., Cox, D.L., Luneau, B., Iwere, F., 2011. Integrated reservoir modeling of a Pinedale tight gas reservoir in the Greater Green River Basin, Wyoming. In: Ma, Y.Z., LaPointe, P. (Eds.), Uncertainty Analysis and Reservoir Modeling. AAPG Memoir 96, Tulsa.

Ma, Y.Z., Seto, A., Gomez, E., 2009. Depositional facies analysis and modeling of Judy Creek reef complex of the Late Devonian Swan Hills, Alberta, Canada. AAPG Bulletin 93 (9), 1235–1256.

Masters, J.A., 1979. Deep basin gas trap, Western Canada. AAPG Bulletin 63 (2), 152.
Meckel, L.D., Thomasson, M.R., 2008. Pervasive tight gas sandstone reservoirs: an overview. In: Cumella, S.P., Shanley, K.W., Camp, W.K. (Eds.), Understanding, Exploring, and Developing Tight Gas Sands, AAPG Hedberg Series, vol. 3, pp. 13–27. Tulsa, OK.
Naik, G.C., 2003. Tight gas reservoirs–an unconventional natural energy source for the future. Retrieved from: www.sublette-se.org/files/tight_gas.pdf.
Pilisi, N., Wei, Y., Holditch, S.A., 2010. Selecting Drilling Technologies and Methods for Tight Gas Sand Reservoirs. Society of Petroleum Engineers. http://dx.doi.org/10.2118/128191-MS. Paper SPE 128191, presented at the 2010 IADC/SPE Drilling Conference in New Orleans, Louisiana, USA, 2–4 Febraury.
Pranata, H.M., Su, W., Huang, B., Li, J., et al., 2014. A Horizontal Drilling Breakthrough in Developing 1.5 m Thick Tight Gas Reservoir. Paper IPTC 17486, presented at the IPTC, Doha Qatar, January 20–22, 2014.
Rogner, H.H., 1997. An assessment of world hydrocarbon resources. Annual Review of Energy and the Environment 22, 217–262.
Rushing, J.A., Newsham, K.E., Blasingame, T.A., 2008. Rock Typing – Keys to Understanding Productivity in Tight Gas Sands. SPE 114164.
Schenk, C.J., Pollastro, 2002. Natural Gas Production in the United States. US Geological Survey Fact Sheet FS-113-01, 2 p.
Schmoker, J.W., 2005. U.S. Geological survey assessment concepts for continuous petroleum accumulations. In: Chapter 13 of Petroleum Systems and Geologic Assessment of Oil and Gas in the Southwestern Wyoming Province, Wyoming, Colorado and Utah. U.S. Geological Survey Digital Data Series DDS-69-D.
Shanley, K.W., 2004. Fluvial Reservoir Description for a Giant Low-permeability Gas Field, Jonah Field, Green River Basin, Wyoming, in AAPG Studies in Geology #52, pp. 159–182.
Shanley, K.W., Cluff, R.M., Robinson, J.W., 2004. Factors controlling prolific gas production from low-permeability sandstone reservoirs. AAPG Bulletin 88 (8), 1083–1121.
Spencer, C.W., 1989. Review of characteristics of low permeability gas reservoirs in western United States. AAPG Bulletin 73 (5), 613–629.
Webb, J.C., Cluff, S.G., Murphy, C.M., Pyrnes, A.P., 2004. Petrology, Petrophysics of the Lance Formation (Upper Cretaceous), American Hunter, Old Road Unit 1, Sublette County, Wyoming, in AAPG Studies in Geology #52 pp.183–213.
Wei, Y.N., Cheng, K., Holditch, S.A., 2009. Multicomponent advisory system can expedite evaluation of unconventional gas reservoirs. In: SPE 124323, SPE Annual Technical Conference and Exhibition, New Orleans, LA, USA, October 4–7, 2009.
Wei, Y., Cheng, K., Jin, X., Wu, B., Holditch, S.A., 2010. Determining Production Casing and Tubing Size by Satisfying Completion Stimulation and Production Requirements for Tight Gas Sand Reservoirs. Paper SPE 132541, presented at the SPE Tight Gas Completions Conference, San Antonio, Texas, USA, November 2–3, 2010.
Wei, Y., Xu, J., 2015. Development of liquid-rich tight gas sand plays - granite wash example. In: Ma, Y.Z., Holditch, S., Royer, J.J. (Eds.), Unconventional Resource Handbook: Evaluation and Development. Elsevier.
Wolff, M., Pelissier-Combescure, J., 1982. FACIOLOG - automatic electrofacies determination. In: Proceeding of Society of Professional Well Log Analysts Annual Logging Symposium, Paper FF.

APPENDIX: METHODS FOR 3D LITHOFACIES MODELING

A1 INDICATOR KRIGING AND SEQUENTIAL INDICATOR SIMULATION (SIS)

Because an indicator variable represents a binary state with two possible outcomes: presence or absence, the indicator variable for three or more lithofacies can be defined in terms of one lithofacies and all others combined to indicate the absence of that selected lithofacies. Each of the lithofacies is analyzed in its turn so that all the lithofacies can be modeled accordingly.

Indicator kriging was initially developed as a nonparametric estimation of spatial distribution (Journel, 1983); it provides a least-square estimate of the conditional cumulative distribution function (ccdf) at a cutoff value for a continuous variable. However, it is now more often used for modeling categorical variables, such as lithofacies. Consider $\boldsymbol{k}$ mutually exclusive lithofacies or rock types; as any location can only have one lithofacies, $\boldsymbol{k}$, its probability can be estimated using simple indicator kriging (Deutsch and Journel, 1991, p. 73, p. 148):

$$\boldsymbol{I}^*(\boldsymbol{x}) = \boldsymbol{Prob}\{\boldsymbol{I_k}(\boldsymbol{x}) = \boldsymbol{1}\} = \boldsymbol{p_k} + \sum \boldsymbol{w_i}[\boldsymbol{I_k}(\boldsymbol{x_i}) - \boldsymbol{p_k}] \tag{A.1}$$

where $\boldsymbol{p_k}$ is the overall or global proportion of the lithofacies $\boldsymbol{k}$, $\boldsymbol{w_i}$ is the weight of the datum $\boldsymbol{i}$, and $\boldsymbol{I_k}(\boldsymbol{x_i})$ is the state of the indicator variable at $\boldsymbol{x_i}$, i.e., the presence or absence of lithofacies, $\boldsymbol{k}$. In other words, the probability of a lithofacies is estimated by a linear estimator, including its global proportion, and the neighboring data. This equation can be solved using simple kriging system:

$$\sum \boldsymbol{w_i c_{ij}} = \boldsymbol{c_{0j}} \quad \text{for } \boldsymbol{i} = 1, \ldots, n \tag{A.2}$$

where $\boldsymbol{C_{ij}}$ and $\boldsymbol{C_{0j}}$ are the indicator covariances of the indicator variables for the lag distances between $\boldsymbol{x_i}$ and $\boldsymbol{x_j}$, and $\boldsymbol{x_0}$ and $\boldsymbol{x_j}$, respectively. The relationship between indicator covariance and indicator variogram for a stationary indicator random function is the same as the general relationship between covariance function and variogram, i.e.,

$$Covariance\ (h) = Variance - Variogram\ (h) \tag{A.3}$$

While indicator kriging is rarely used in reservoir modeling, its stochastic simulation counterpart is commonly used for modeling lithofacies and rock type. This section discusses indicator variogram and sequential indicator simulation for modeling lithofacies.

A1.1 Indicator Variogram

Indicator variograms of lithofacies often show a second-order stationarity with a definable plateau (Jones and Ma, 2001). A lithofacies variogram observed across stratigraphic formations is typically cyclical as a function of lag distance. This has been termed a hole-effect variogram in geostatistics (Jones and Ma, 2001). Cyclicity and amplitudes in hole-effect variograms are strongly affected by relative abundance of each lithofacies and by the variation in the sizes of lithofacies bodies.

Sample density is very important for accurately describing an experimental variogram (Ma et al., 2009). In a reservoir with low sandstone fraction, if individual sandstone or other lithofacies bodies are sampled densely enough, the experimental variogram will likely show spatial correlations, possibly with cyclicity. However, if individual lithofacies bodies are sampled with only one observation each, the experimental indicator variogram will likely fluctuate around a plateau even for short lag distances, and thus appear as nugget effect. Geology is not random, but a sparse sampling can make it appear random. An experimental variogram calculated from data typically is fitted into a theoretical model, such as a spherical or exponential function, possibly with a partial nugget effect. The larger the relative proportion of the nugget effect, the more random will be the lithofacies model. The cyclicity of lithofacies in spatial distributions, vertical or horizontally, can be better modeled using a hole-effect variogram.

A1.2 Sequential Indicator Simulation (SIS)

SIS simulates the indicator variable sequentially, and it is basically the categorical-variable simulation counterpart of sequential Gaussian simulation, which is for continuous-variable simulation (Deutsch and Journel, 1991). For simulating lithofacies, at each grid cell, indicator kriging is first carried out according to Eqs (A.1) and (A.2); an ordering of the lithofacies is then defined, which also defines a cdf-type scaling of the probability interval between 0 and 1; this is followed by drawing a random number and determining the simulated lithofacies at the location. This process is repeated following a random path until all the grid cells are simulated. The previously simulated data and original data are both used in indicator kriging (Eq. (A.2)), when they are within the defined neighborhood, for conditioning the simulation.

A2 OBJECT-BASED MODELING

One of the most commonly used object-based modeling (OBM) methods is the fluvial object-based modeling, which generates channels with defined ranges in width, thickness, and sinuosity (Clement et al., 1990; Holden et al., 1997). Channels can also be modeled in association with attached crevasses/splays that can have defined ranges of width and thickness. The fluvial channel parameters defined for OBM include uncertainty ranges, based on the regional geology, seismic attribute analysis, fluvial depositional analogs, and sedimentology of the basin. An example of defining parameters in modeling meandering fluvial channels in Pinedale of the Greater Green River Basin can be found in Ma et al. (2011).

More general OBM uses the user-defined objects. The shape of the objects typically include ellipse, half ellipse, quart ellipse, pipe, lower half pipe, upper half pipe, box, fan lobe, Aeolian sand dune, and oxbow lake. Some of these objects can be modeled with a specified profile, such as rounded, rounded base, rounded top, or sharp edges. The object shapes should be determined based on the depositional characteristics.

A3 TRUNCATED GAUSSIAN SIMULATION

Some depositional environments show a clear orderly lithofacies transition; SIS can attempt to model the transition through the use of probability maps, but the SIS models often do not replicate the transition satisfactorily. The truncated Gaussian simulation (TGS) can be used for modeling the lithofacies transition more aptly. This method can ensure consistency of the indicators variograms and cross variograms in the model (Galli et al., 1994). Often a facies transition represents a nonstationarity, but truncated Gaussian method can deal with the nonstationarity of lithofacies both laterally and vertically.

Before the TGS simulation, the facies codes are transformed into continuous normal score space using cutoffs on a cumulative distribution function. The transform is based on the facies code and the probability of the facies (the target fraction for the facies if no trend is specified). TGS then performs a Gaussian random function simulation or sequential Gaussian simulation (SGS) on normal-scored continuous values. In theory, the spherical variogram, which is the most commonly used variogram, cannot be used for this method.